THE

PHYSICAL REVIEW

A journal of experimental and theoretical physics established by E. L. Nichols in 1893

SECOND SERIES, VOL. 182, NO. 4 20 JUNE 1969

Optical-Model Analysis of Nucleon Scattering from 1*p*-Shell Nuclei between 10 and 50 MeV*†

B. A. WATSON‡§

Argonne National Laboratory, Argonne, Illinois 60439 and *Indiana University, Bloomington, Indiana 47401*

AND

P. P. SINGH

Indiana University, Bloomington, Indiana 47401

AND

R. E. SEGEL

Argonne National Laboratory, Argonne, Illinois 60439 and *Northwestern University, Evanston, Illinois 60200*

(Received 14 February 1969)

Differential cross sections for protons scattered from B^{10} were measured and, combined with published differential cross sections and polarizations for protons elastically scattered from Li^6, Li^7, Be^9, B^{10}, B^{11}, C^{12}, C^{13}, N^{14}, and O^{16} at bombarding energies between 10 and 50 MeV, are analyzed in terms of the optical model. An investigation of the systematic effects observed in applying the optical model to light nuclei reveals two peculiarities. First, an examination of the effects of a nonlocal potential indicates that the radius parameter of the real central potential is energy-dependent. Second, the Thomas form usually used for the spin-orbit potential is shown to lose its surface-peaked character in the case of light nuclei; but a proposed slight modification avoids this defect. The set of parameters found to give a good description of the data over a range of incident nucleon energy and target mass was shown to be similar to the sets of parameters found to describe the nucleon scattering from heavy nuclei. Using the prescriptions for the parameters of the present study but reversing the signs of the $(N-Z)/A$ terms leads to fits of comparable quality to the differential cross sections for 14-MeV neutrons scattered from Li^7, Be^9, B^{11}, and N^{14}.

I. INTRODUCTION

FOR heavy nuclei and bombarding energies above 10 MeV, Perey[1] and others[2–4] have shown that the optical model gives a satisfactory description of the elastic scattering of nucleons. The model has not enjoyed equal success in its application to light nuclei.[4] One of the most exhaustive studies[5] involved proton scattering from C^{12} at bombarding energies up to 20 MeV. While any individual angular distribution could be reproduced, the model parameters fluctuated wildly as a function of energy. This result was not surprising since yield curves[6] for protons scattered from C^{12} show that resonant structures are dominant in this energy range. Behavior of this type indicates that some of the basic assumptions of the model may be violated. First, even at fairly high excitations the density of compound-nucleus levels is low for light nuclei and hence the nuclear-structure effects which the optical model cannot describe are not sufficiently averaged out. Second, it may not be appropriate to replace the nucleus with a potential having a simple radial form (e.g., a Woods-Saxon form which is often used in the case of heavy nuclei). Inherent in a replacement of this kind is the assumption that the nucleus can be regarded as a con-

* Work partially supported by the U.S. Atomic Energy Commission and the National Science Foundation.
† Summary of part of a thesis presented by B. A. Watson to the Department of Physics, Indiana University, 1968.
‡ Present address: Stanford University, Stanford, Calif.
§ AMU-ANL predoctoral fellow.
[1] F. G. Perey, Phys. Rev. **131**, 745 (1963).
[2] L. Rosen, J. G. Beery, A. S. Goldhaber, and E. H. Auerbach, Ann. Phys. (N.Y.) **34**, 96 (1965); B. Buck, Phys. Rev. **130**, 712 (1963).
[3] M. P. Fricke, E. E. Gross, B. J. Morton, and A. Zucker, Phys. Rev. **156**, 1027 (1967).
[4] P. E. Hodgson, Ann. Rev. Phys. **17**, 1 (1967).
[5] J. S. Nodvik, C. B. Duke, and M. A. Melkanoff, Phys. Rev. **125**, 975 (1962).
[6] G. G. Shute, D. Robson, V. R. McKenna, and T. A. Berztiss, Nucl. Phys. **37**, 635 (1962); J. K. Dickens, D. A. Haner, and C. N. Waddell, Phys. Rev. **132**, 2159 (1963).

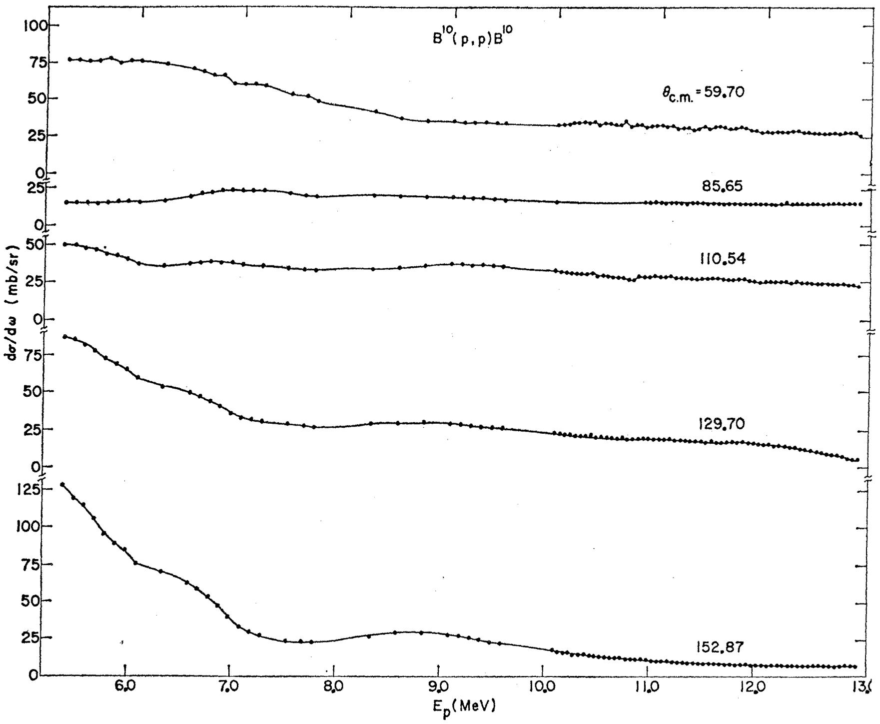

FIG. 1. Excitation functions of protons elastically scattered from B^{10}.

tinuous distribution of nuclear matter to the incident particle. There are so few nucleons in light nuclei that this approximation may not be valid.

In this study, the optical model has been reexamined to assess its applicability to light nuclei. The main objective of the analysis was to explore the possibility of finding a set of optical parameters that would reproduce the general features of nucleon scattering from light nuclei. The general spirit of the optical model is that it should describe the average properties of nucleon scattering, both with respect to energy of the incident particle and with respect to the mass of the target. Thus, if any meaningful conclusions were to be drawn from the results, it was considered mandatory that the parameters vary smoothly with bombarding energy and that they give a reasonable description of nucleon scattering from several nuclei.

II. EXPERIMENTAL DATA

The measurements made in the present investigation include angular distributions in 100–200-keV steps and excitation functions in 100-keV steps at $\theta_{c.m.}=59.70°$, 85.65°, 110.54°, 129.70°, and 152.87° for protons elastically scattered from B^{10} over the proton energy range of 5.0–13.4 MeV. The experimental details are outlined elsewhere.[7] Figure 1 shows the excitation functions and Figs. 2 and 3 show the differential cross sections. The solid lines are smooth curves through the data points. The experimental uncertainty, excluding absolute normalization, is of the order of the size of the plotted points and the absolute normalization was determined to within $\pm 20\%$.[7] The only resonant-type structure appearing in the yield curves is a broad resonance centered at about 5.0 MeV. The angular distribution data were recorded in 5° steps from 25° to 170°. The angular distributions have diffraction-type structure typical of a direct interaction. Below $E_p=6.5$ MeV, there is one minimum in the angular pattern near 85° and its position is independent of bombarding energy. From 6.5 to 13.4 MeV, the angular distributions have two minima, one at 80° and the other at 145°.

The characteristics of the yield curves and the angular distributions suggested that the optical model might be able to describe the experimental data. We subsequently found a set of parameters that gave a good description of the data from 8.0 to 13.4 MeV. This led to the question whether these parameters, with perhaps some small modifications, could account for the scattering of nucleons from other $1p$-shell nuclei.

The present analysis incorporates proton and neutron elastic-scattering data for several $1p$-shell nuclei at bombarding energies between 10 and 50 MeV. The type and source of the data are summarized in Table I. Most of the proton angular-distribution data cover an angular range of approximately 30°–165° in angular steps of 5°–10°. The uncertainties in the relative cross sections are usually about 2%, those in the absolute normalization are of the order of 15%. The cross sec-

[7] For details, see B. A. Watson, Argonne National Laboratory Physics Division Informal Report No. 1968B (unpublished); and B. A. Watson, R. E. Segel, J. J. Kroepfl, and P. P. Singh, Phys. Rev. (to be published).

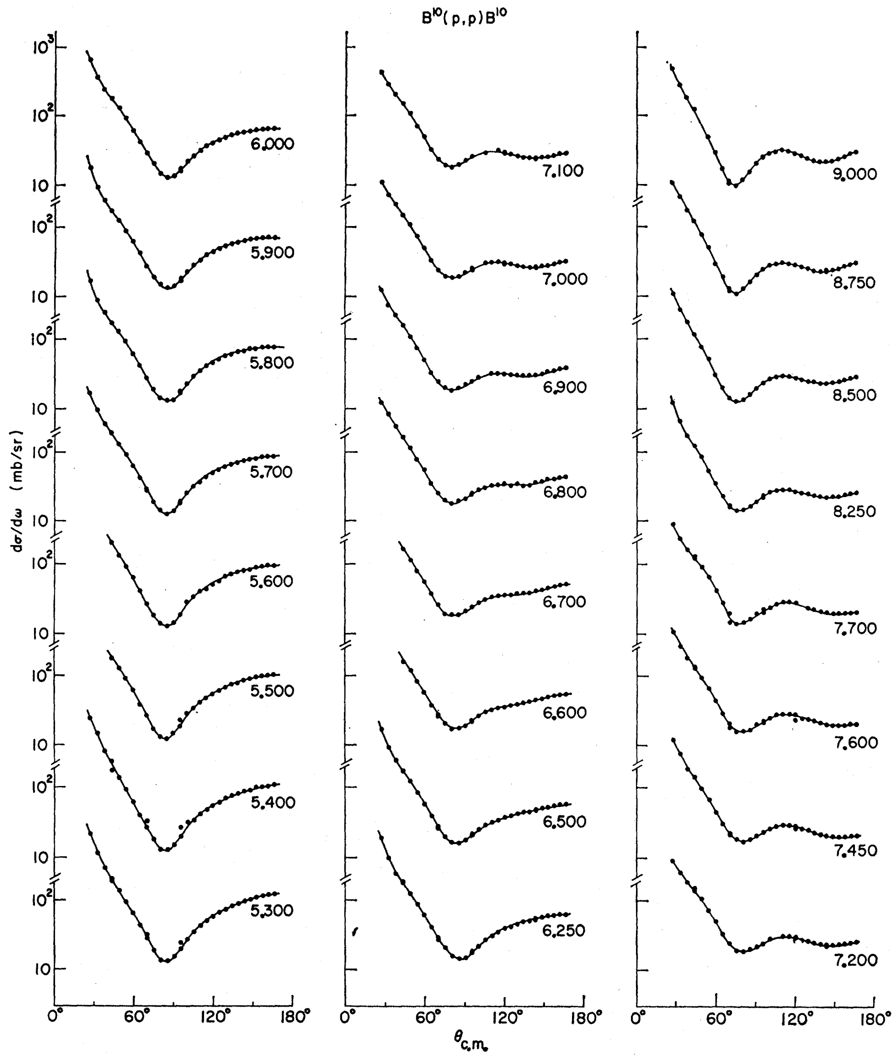

FIG. 2. Differential cross sections for protons elastically scattered from B^{10} for bombarding energies between 5.3 and 9.0 MeV.

tions usually vary smoothly as a function of nucleon energy; the low-energy C^{12} cross sections are the exception. At high energies ($E_p>30$ MeV), the cross sections for all nuclei have less pronounced structure than at low energies ($E_p<30$ MeV). The neutron-scattering cross sections have been reported only at the bombarding energy of 14 MeV. The absolute and relative uncertainties in these measurements are of the order of 20%. The proton polarizations include data for 1p-shell nuclei at varying energies between 10 and 50 MeV.

III. NUMERICAL CONSIDERATIONS

The optical potential used had a form similar to that used in other analyses,[2–4] namely,

$$V_{\mathrm{opt}}=-V_R f(r,r_R,a_R)+iW_V f(r,r_I,a_I)$$
$$+4ia_I W_S(d/dr)f(r,r_I,a_I)+\boldsymbol{\sigma}\cdot\mathbf{l}V_{\mathrm{so}}\left(\frac{\hbar}{m_\pi c}\right)^2\frac{1}{r_{\mathrm{so}}A^{1/3}}\frac{d}{dr}f(r,r_{\mathrm{so}},a_{\mathrm{so}})+V_{\mathrm{Coul}}(r,r_c),$$

where f is the usual Woods-Saxon form factor

$$f(r,r_0,a_0)=\{1+\exp[(r-r_0A^{1/3})/a_0]\}^{-1},$$

and the Coulomb potential V_{Coul} was that of a uniformly charged sphere, namely,

$$V_{\mathrm{Coul}}=(zZe^2/2R_c)(3-r^2/R_c^2),\qquad \text{for } r\leq R_c=r_cA^{1/3}$$
$$=(zZe^2/r),\qquad \text{for } r>R_c$$

z and Z being the charges of the incident and target particles, respectively.

There is evidence that the effective nucleon-nucleus interaction is nonlocal.[1,8] An investigation was undertaken to determine if any peculiarities in the local potentials for light nuclei might arise as a result of the

[8] F. Perey and B. Buck, Nucl. Phys. 32, 353 (1962).

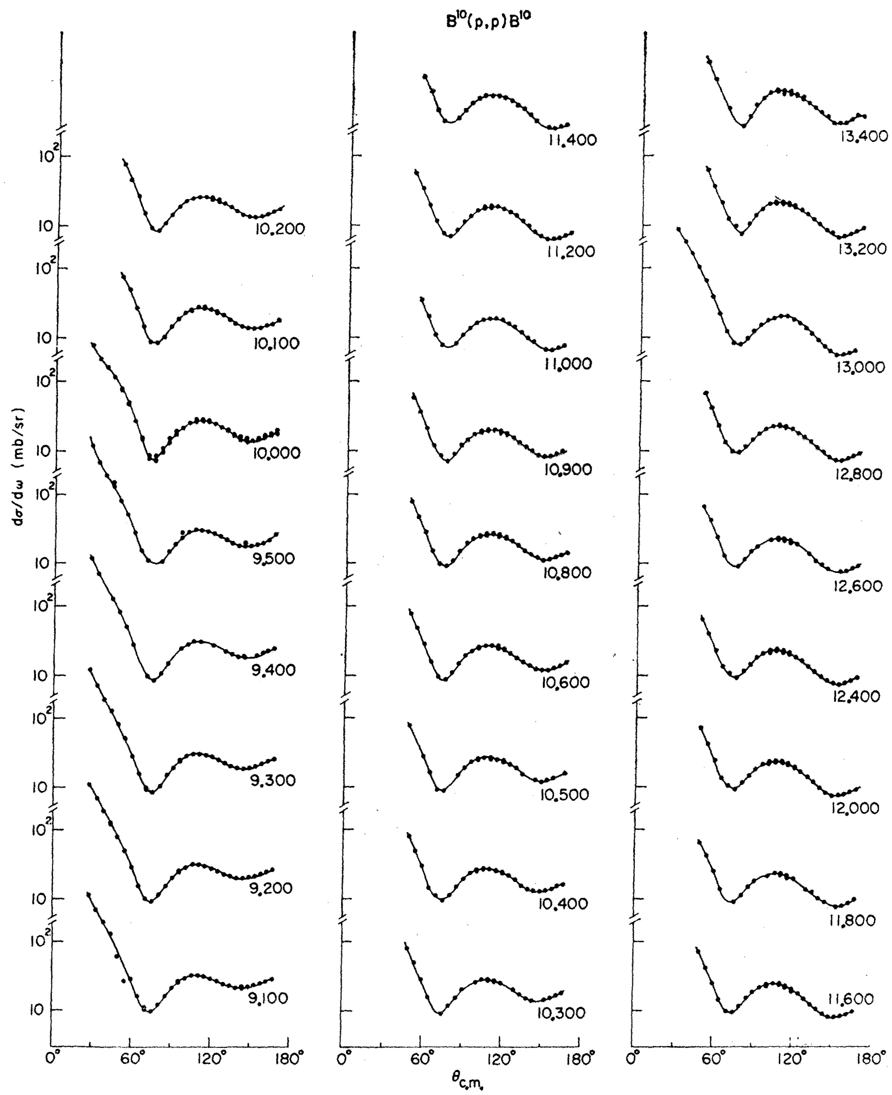

FIG. 3. Differential cross sections for protons elastically scattered from B^{10} for bombarding energies between 9.1 and 13.4 MeV.

nonlocal nature of nucleon-nucleus interaction. The program used for this purpose was one for neutron scattering, written by Elwyn and Monahan of Argonne National Laboratory,[9] which employs the approximate expressions of Perey and Buck.[10] Given a set of nonlocal parameters, the program calculates local-potential parameters for a given neutron bombarding energy. It is assumed that the spin-orbit potential can be treated in the local approximation and, thus, does not enter into the calculation. Since the spin-orbit potential is small in comparison with the real central potential, its omission should not significantly affect the results. For proton scattering, the Coulomb potential must be considered. Sood[11] investigated the problem in detail and found that the main effect is to increase the strength of the real potential by a term proportional to the charge of the target. Thus, the general energy dependence that nonlocal effects introduce into the local potential are similar for neutrons and protons.

The nonlocal-potential parameters used for these sample calculations were

$$V=70 \text{ MeV}, \quad r_0=1.25 \text{ F}, \quad a=0.65 \text{ F},$$

$$W=15 \text{ MeV}, \quad \beta=0.9 \text{ F},$$

where the real potential was given a volume form and

[9] A. Elwyn and J. E. Monahan (private communication).

[10] It should be noted that the potential suggested by Perey and Buck is of a special kind, and it is not yet known whether this particular form is appropriate to actual nuclei.

[11] P. C. Sood, Nucl. Phys. 84, 106 (1966).

TABLE I. Summary of the type and source of the data included in the optical-model analysis.

Reaction	Incident energy (MeV)	Type of measurement	Ref.
Li^6+p	12.0	Ang. dist.	a
	19.6	Ang. dist.	b
	39.7	Ang. dist.	c
	50.0	Ang. dist. and polarization	d
Li^7+p	14.5	Polarization	e
	19.6	Ang. dist.	b
	39.7	Ang. dist.	c
	50.0	Ang. dist. and polarization	d
Li^7+n	14.0	Ang. dist.	f
Be^9+p	$5.0\leq E_p\leq 15.0$	Ang. dist.	g
	11.4	Polarization	h
	18.88	Ang. dist.	i
	30.3	Ang. dist. and polarization	j
Be^9+n	14	Ang. dist.	k
$B^{10}+p$	$5.5\leq E_p\leq 13.0$	Ang. dist.	l
	10.0	Polarization	h
	17.9	Ang. dist.	m
$B^{11}+p$	$12\leq E_p\leq 20.5$	Ang. dist.	n
$B^{11}+n$	14.0	Ang. dist.	o
$C^{12}+p$	$12\leq E_p\leq 20.$	Ang. dist.	p
	31.0	Ang. dist.	q
	40.0 and 50.0	Ang. dist.	r
	30, 40, 50	Polarization	r
$C^{13}+p$	14.5	Polarization	e
$N^{14}+p$	9.73	Ang. dist.	s
	10.4	Polarization	h
	19.9	Ang. dist.	t
	31.0	Ang. dist.	u
$N^{14}+n$	14.0	Ang. dist.	v
$O^{16}+p$	$30\leq E_p\leq 46$	Ang. dist. and polarization	w

[a] W. D. Harrison and A. Bruce Whitehead, Phys. Rev. **132,** 2607 (1963).
[b] R. A. Vanetsian, A. P. Klycharen, and E. D. Fedchenko, Soviet J. At. Energy **6,** 490 (1960).
[c] Sheau-Wu Chen and Norton M. Hintz, in *International Conference on Nuclear Forces and the Few Nucleon Problem*, edited by T. C. Griffith and E. A. Power (Pergamon Press, Inc., New York, 1960), p. 683.
[d] G. S. Mani, A. D. B. Dix, D. T. Jones, and M. Richardson, Rutherford Laboratory Report No. RHEL/R-136, 1967, p. 49 (unpublished).
[e] L. Rosen and W. T. Leland, Phys. Rev. Letters **8,** 379 (1962).
[f] Alice H. Armstrong, Juanita Gammel, L. Rosen, and Glenn M. Frye, Jr., Nucl. Phys. **52,** 505 (1964).
[g] F. W. Bingham, M. K. Brussel, and T. D. Steben, Nucl. Phys. **55,** 256 (1964).
[h] L. Rosen, J. E. Brolley, Jr., and L. Stewart, Phys. Rev. **121,** 1423 (1961).
[i] I. E. Dayton and G. Schrank, Phys. Rev. **101,** 1358 (1956).
[j] M. J. Kenny, J. Lowe, D. L. Watson, and H. Wojciechowski, Ref. d, p. 31.
[k] M. P. Nakada, J. D. Anderson, C. C. Gardner, and C. Wong, Phys. Rev. **110,** 1439 (1958).
[l] Present work.
[m] G. Schrank, E. K. Warburton, and W. W. Daehnick, Phys. Rev. **127,** 2159 (1962).
[n] R. H. Siemssen, M. Rickey, and L. L. Lee, Jr. (private communication).
[o] K. Tesch, Nucl. Phys. **37,** 412 (1962).
[p] Y. Nagahara, J. Phys. Soc. Japan **16,** 133 (1961); R. W. Peele, Phys. Rev. **105,** 1311 (1957).
[q] J. Kirk Dickens, David A. Haner, and Charles N. Waddell, Phys. Rev. **129,** 743 (1963).
[r] E. J. Burge, M. Calderbank, J. A. Fannon, V. E. Lewis, A. A. Rush, D. A. Smith, and N. K. Ganguly, in Ref. d, p. 41.
[s] N. M. Hintz, Phys. Rev. **106,** 1201 (1957).
[t] R. H. Chow and B. J. Wright, Can. J. Phys. **35,** 184 (1957).
[u] C. C. Kim, S. M. Bunch, D. W. Devins, and H. H. Forster, Nucl. Phys. **58,** 32 (1964).
[v] R. Bauer, J. D. Anderson, and L. Christensen, Nucl. Phys. **48,** 152 (1963).
[w] J. Cameron, University of California at Los Angeles Technical Report No. P-80, 1967 (unpublished).

the imaginary potential a surface form. Most of the calculations were performed for neutrons scattered from B^{10}. The results in Fig. 4 show that the parameters for the equivalent local potential decrease as a function of energy. In this figure, the points represent the calculated values for the parameters of the local potential and the solid lines are smooth curves through the points. Over an energy range of 15 MeV the decrease in the parameters is, to a good approximation, linear; but over larger energy regions the departure from linearity is noticeable. The lower graph of Fig. 5 is a semilogarithmic plot of the strength of the real potential over a 200-MeV range of nucleon energy. As previously noted by Sood[11] and by Gersten,[12] the energy dependence over this large a range can best be expressed as an exponential.

The energy dependence of the diffuseness parameter is very small—certainly not large enough to be experimentally observed (as can be seen in Fig 4) The change in the diffuseness parameter in going from 0- to

[12] A. Gersten, Nucl. Phys. **A96,** 288 (1967).

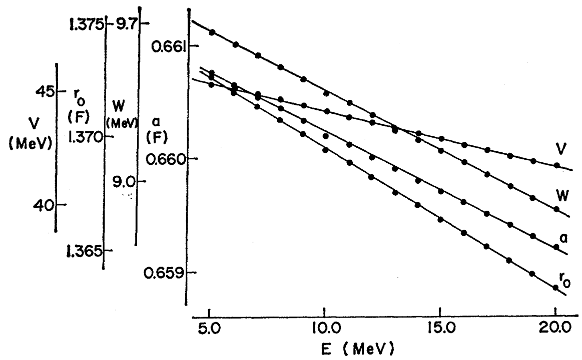

FIG. 4. Optical parameters of a local potential calculated from a nonlocal potential.

200-MeV bombarding energy was calculated to be less than 1%.

The energy dependence calculated for the radius parameter of the real central potential is shown in the upper graph of Fig. 5. This variation with energy can be fitted by

$$r_0(E)=r_0'-(\alpha/A^{1/3})E,$$

where α is independent of the mass A of the target and r_0' is independent of energy. The energy dependence of the radius $R=r_0(E)A^{1/3}$ of the Woods-Saxon well can then be expressed as $R=R_0-\alpha E$, where $R_0=r_0'A^{1/3}$. Thus, for light nuclei the change in R with energy would be much more noticeable than for heavy nuclei, since α/R_0 is larger for light nuclei than it is for heavy nuclei.

To see the effect of an energy dependence of the radius parameter of the real central potential, we examined the energy dependence of the product $V_RR_R^2$, where V_R is the strength of the real central potential. Then if V_R and R_R have the quasilinear energy dependence $V_R=V_0-\gamma E$ and $R_R=R_0-\alpha E$, the product $V_RR_R^2$ is given by

$$V_RR_R^2=V_0R_0^2-(\gamma R_0^2+2\alpha R_0V_0)E+(2\alpha\gamma R_0+\alpha^2V_0)E^2-\alpha^2\gamma E^3.$$

For heavy nuclei the γR_0^2 term dominates the energy variation and consequently $V_RR_R^2$ is (to a good approximation) a linear function of energy. In going to lighter nuclei, however, γR_0^2 decreases as the $\frac{2}{3}$ power of the target mass A, while the term α^2V_0 in the coefficient of E^2 is independent of A. Thus, an E^2 component could become noticeable for light nuclei if the data cover a large energy range.[13]

The energy dependence of the radius parameter may also be reflected through the mean-square (ms) radius of the central potential. Greenlees *et al.*[14] have developed a reformulation of the optical model in which the real parts of the potential are obtained from nuclear-matter distributions and the nucleon-nucleon force. The nuclear-matter distribution is assumed to have a Woods-Saxon radial dependence for which the radius R_m and the diffuseness parameter a_m are determined by analysis of the proton-scattering cross sections. They found that the ms radius of the matter distribution is much better determined than are the parameters R_m and a_m. The ms radius of a Woods-Saxon distribution is related to the parameters r_0 and a by the approximate expression[15] $\langle r^2\rangle=R_0^2[0.6+13.89(a/R_0)^2]$, where $R_0=r_0A^{1/3}$. To a good approximation the ms radius $\langle r_m^2\rangle$ of the mass distribution is related[14] to the ms radius $\langle r_R^2\rangle$ of the real potential by $\langle r_R^2\rangle=\langle r_m^2\rangle+3$.[16] Therefore, the ms radius of the real central potential should be well determined by fitting the experimental cross sections. Since the radius parameter is expected to change with energy, the ms radius $\langle r_R^2\rangle$ should change as the energy of the incident particle changes. Because of the $V_RR_R^2$ ambiguity, it might be expected that an energy dependence in the radius parameter could be compensated by an increased energy dependence in the strength of the real potential (if the product $V_RR_R^2$ is approximately a linear function of the energy). Since the optical parameters required for a best fit to the experimental data should reflect a sensitivity to the ms radius $\langle r_R^2\rangle$ and since $\langle r_R^2\rangle$ is only a function of the

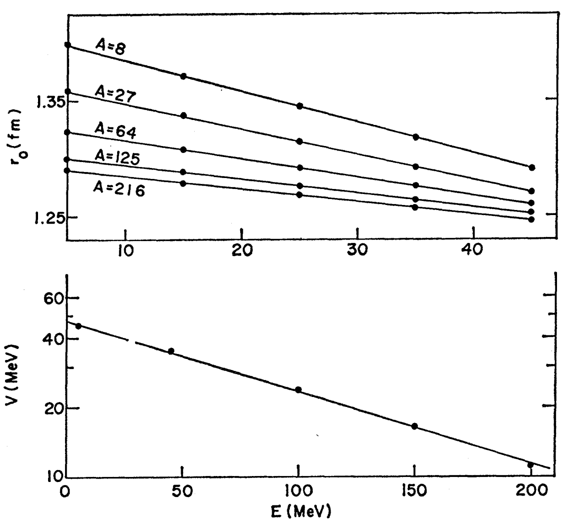

FIG. 5. Energy dependence (above) of the radius parameter r_0 of the real central potential for different values of the mass A of the target and (below) of the strength V of the real central potential resulting from a nonlocal potential.

[13] G. R. Satchler, L. W. Owen, A. J. Elwyn, G. L. Morgan, and R. L. Walter have also used [Nucl. Phys. **A112**, 1 (1968)] an energy-dependent radius in the optical-model analysis of nucleon scattering from He^4.

[14] G. W. Greenlees, G. J. Pyle, and Y. C. Tang, Phys. Rev. Letters **17**, 33 (1966); and Phys. Rev. **171**, 1115 (1968).

[15] L. R. B. Elton, *Introductory Nuclear Theory* (Pitmans, London, 1949), p. 150.

[16] Exact value of the difference $\langle r_R^2\rangle-\langle r_m^2\rangle$ is not yet established. For example, see D. Slanina and H. McManus, Nucl. Phys. **A116**, 271 (1968).

radius parameter r_0 and the diffuseness a, however, an energy dependence in the radius parameter could not be counterbalanced by changing the energy dependence of the strength of the real central potential. Further, because the results of the nonlocal-potential calculations indicate that the radius parameter should be more energy-dependent for light nuclei than for heavy nuclei, the change in $\langle r_R^2 \rangle$ for light nuclei should be more significant than that for heavy nuclei.

For light nuclei, a question arises concerning the spin-orbit potential. For heavy nuclei, the radial part of the spin-orbit potential is taken to have the Thomas form

$$V_{\rm so}(r) \propto \boldsymbol{\sigma}\cdot\mathbf{l}V_{\rm so}(\hbar/m_\pi c)^2 r^{-1}(d/dr)\rho(r),$$

where $\rho(r)$ is the density distribution of nuclear matter. It is assumed that $f_R(r) \propto \rho(r)$, where $f_R(r)$ is the radial form factor of the real central potential. The theoretical justification of this form, discussed by Blin-Stoyle[17] and Greenlees,[14] is not clear cut because the exact origin of this force is not known. The fact that its radial part is peaked at the surface of the nucleus is considered reasonable since the particles of high angular momentum, which are known to experience the largest splitting, spend most of their time at the surface of the nucleus. For light nuclei the effect may extend into the nucleus but still should be maximum near the surface. For low A, however, the Thomas form (Fig. 6) is dominated by the $1/r$ term and becomes very large at appreciable distances from the origin.[18] A better form would perhaps be

$$V_{\rm so}(r) \approx \boldsymbol{\sigma}\cdot\mathbf{l}V_{\rm so}(\hbar/m_\pi c)^2 R_{\rm so}^{-1}(d/dr)f_R(r),$$

where $R_{\rm so}=r_{\rm so}A^{1/3}$. This radial form is close to the Thomas form for heavy nuclei but retains a surface-peaked characteristic for light nuclei. For heavy nuclei the strength $V_{\rm so}$ required to fit the experimental data should be about the same for either of the above forms.

IV. SEARCH PROCEDURE AND RESULTS

The procedure for finding a good set of parameters consisted in visually comparing the experimental cross sections with those calculated with a given set of parameters, then systematically changing the parameters to see if the fit could be improved. This approach had several advantages. First, the whole body of data could be compared with calculations based on a chosen set of parameters. This was particularly important since there was some question about the mass dependence and energy dependence that the parameters might display. Second, the effects of errors in absolute normalization would not conceal an over-all good reproduction of the general trends in the data. It has been

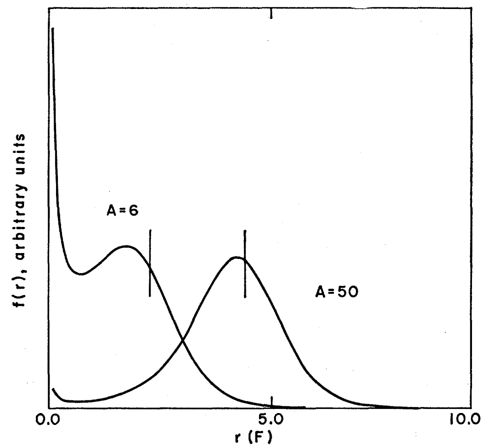

FIG. 6. Radial dependence of the Thomas form of the spin-orbit potential for masses $A=50$ and $A=6$.

shown[1,19] that a small error in absolute normalization has a relatively large effect on the parameters required for a best fit. Since the data came from several sources, it was thought that this could be a significant source of trouble.

In order to make an intelligent guess as to how to change the parameters to get a better fit, we undertook a systematic study to see how each parameter affected the calculated angular distributions and polarizations. For the most part, the effects of each parameter are the same as in the case of heavy nuclei.[19] The one exception was the strength of the spin-orbit potential, which has a pronounced effect on the cross section at large angles ($\theta > 100°$). For low bombarding energies, the strength $V_{\rm so}$ of the spin-orbit potential is the most sensitive control of the position of the second minimum relative to the position of the first minimum. This difference between the sensitivities at high and low energies is probably due to the number of partial waves contributing to the cross section. At high bombarding energies, many partial waves contribute and the correction due to spin-orbit splitting is relatively small. This is not true at low bombarding energies, at which only a few partial waves are involved.

The computer code JIB3, written by F. G. Perey and modified by R. H. Siemssen, was used to perform the calculations. The parameters judged to best fit the experimental data were

$$V_R=60.0+0.4(Z/A^{1/3})\pm 27.0[(N-Z)/A]-0.3E_{\rm c.m.},$$

$$V_{\rm so}=5.5,$$

$$r_R=r_I=r_{\rm so}=r_c=1.15-0.001E_{\rm c.m.},$$

$$a_R=a_{\rm so}=0.57, \qquad a_I=0.5,$$

$$W_s=W_s(E)\pm 10.0(N-Z)/A,$$

$$W_V=W_V(E),$$

[17] R. J. Blin-Stoyle, Phil. Mag. **46**, 973 (1955).

[18] G. R. Satchler has pointed out [Nucl. Phys. **A100**, 497 (1967)] that the centrifugal barrier would counterbalance this divergence. However, its effect may be a little more serious at lower proton energies than at higher energies.

[19] P. E. Hodgsen, *The Optical Model of Elastic Scattering* (Oxford University Press, London, 1963).

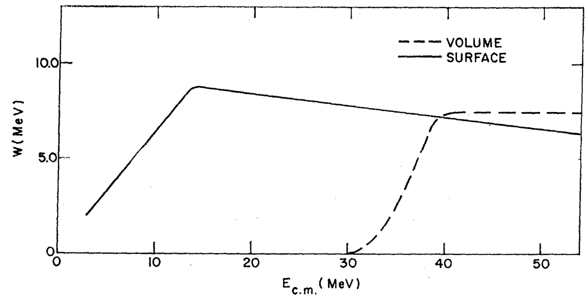

FIG. 7. Energy dependence of the strengths of the volume and surface imaginary potentials as determined by fitting to the experimental cross sections.

where potentials are in MeV, lengths in 10^{-13} cm and + sign is for protons and the − sign for neutrons in the relations for V_R and W_s. For neutron scattering, the term $0.4Z/A^{1/3}$ in V_R drops out.

The energy depencences of the strengths of the imaginary potentials determined in the present study are shown in Fig. 7. To a good approximation, these can be parameterized by

$$
\begin{aligned}
W_S &= 0.64E_{\text{c.m.}}, && \text{for } E_{\text{c.m.}} < 13.8 \text{ MeV}\\
&= 9.60\text{ MeV} - 0.06E_{\text{c.m.}}, && \text{for } E_{\text{c.m.}} \geq 13.8 \text{ MeV}\\
W_V &= 0, && \text{for } E_{\text{c.m.}} < 32.7 \text{ MeV}\\
&= 1.15(E_{\text{c.m.}} - 32.7\text{ MeV}), && \text{for } 32.7 \leq E_{\text{c.m.}} \leq 39.3 \text{ MeV}\\
&= 7.5 \text{ MeV}, && \text{for } E_{\text{c.m.}} > 39.3 \text{ MeV}.
\end{aligned}
$$

The experimental data and calculations based on the parameters shown above are compared in Figs. 8–16. This set of parameters gives a good description of the over-all trends in the data as the mass of the target and the energy of the incident particle are changed. The differential cross sections of protons elastically scattered from Li^6 and Li^7 for bombarding energies between 10 and 50 MeV are shown in Fig. 8. For energies above 30 MeV, the calculations have more pronounced structure than is present in the experimental angular distributions. To a fair degree the optical model calculations reproduce the positions of the first minimum and the general decrease in magnitude of the cross sections with increasing angle. The principal difference is in the absolute magnitude and could be partially due to experimental uncertainties in the absolute normalization. For bombarding energies below 30 MeV, the position of the first minimum is not exactly reproduced, but the shapes are similar to those of the experimental angular distributions. The only

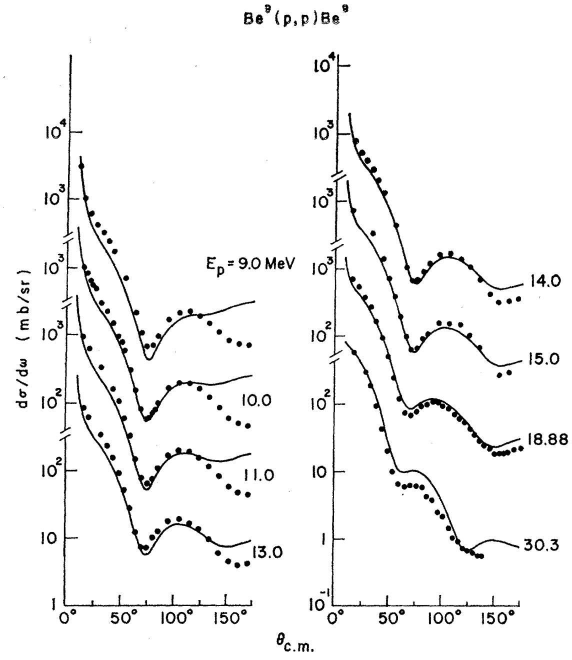

FIG. 9. Differential cross sections of protons scattered from Be^9 compared with the optical-model calculations.

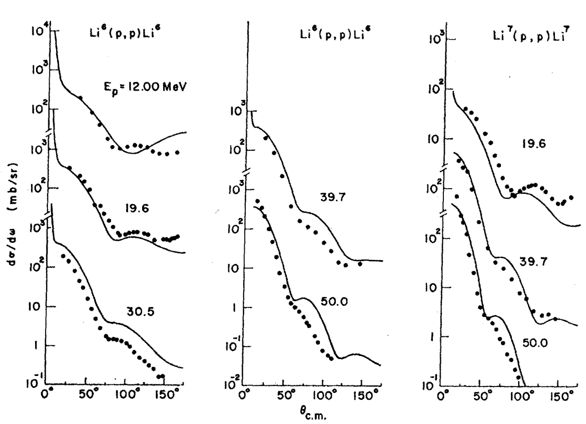

FIG. 8. Differential cross sections of protons scattered from Li^6 and Li^7 compared with the optical-model calculations.

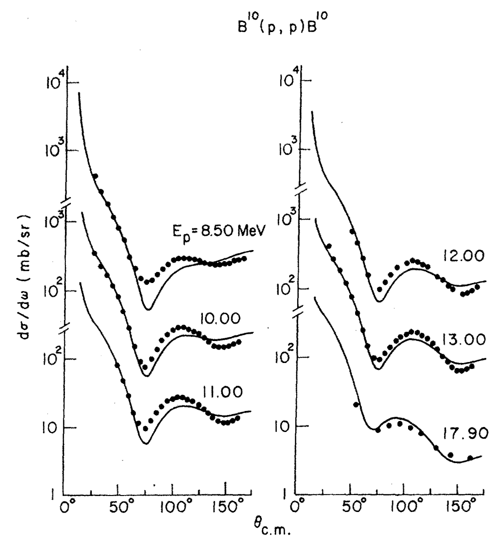

FIG. 10. Differential cross sections of protons scattered from B^{10} compared with the optical-model calculations.

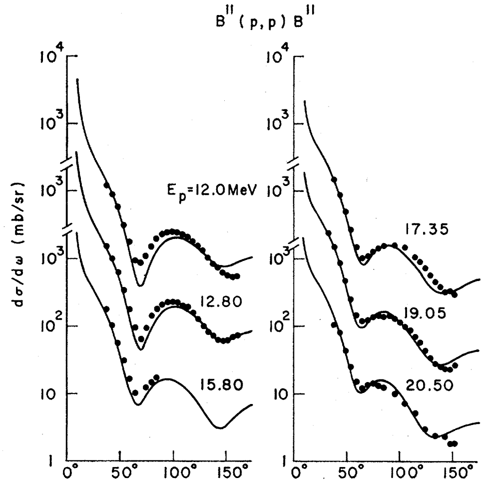

FIG. 11. Differential cross sections of protons scattered from B^{11} compared with the optical-model calculations.

exception is for the angular distribution of 12-MeV protons scattered from Li^6.

The results for 9–30-MeV protons scattered from Be^9 are shown in Fig. 9. For bombarding energies above 13 MeV, the experimental angular distributions are well reproduced by the optical-model calculations. Both the magnitude and the positions of the maxima and minima of the differential cross sections are reproduced over the whole angular range. For bombarding energies between 9 and 13 MeV, the predicted cross sections for back angles ($\theta > 100°$) are greater than the experimental cross sections. The position of the first minimum is reproduced and the calculated magnitudes are in agreement with the experimental cross sections for scattering angles less than 100°.

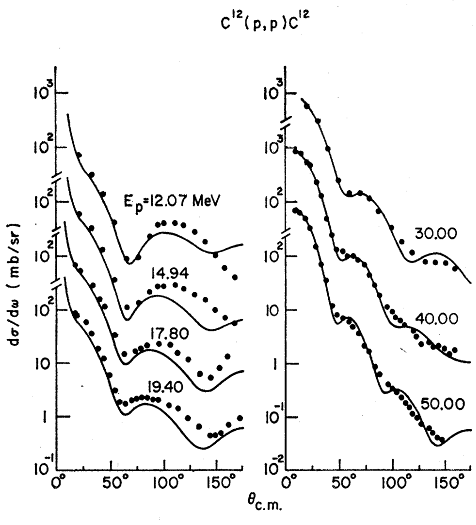

FIG. 12. Differential cross sections of protons scattered from C^{12} compared with the optical-model calculations.

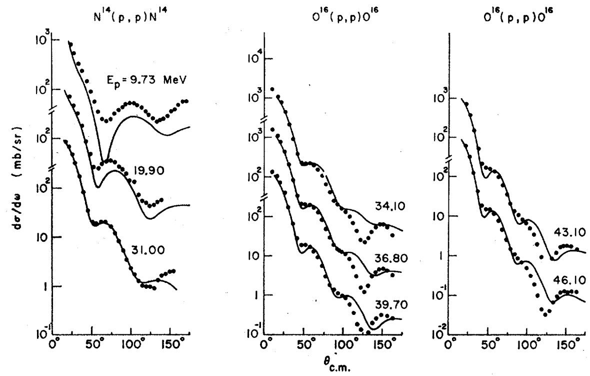

FIG. 13. Differential cross sections of protons scattered from N^{14} and O^{16} compared with the optical-model calculations.

Calculated cross sections for protons with energies between 8.5 and 18.0 MeV scattered from B^{10} are compared with the experimental cross sections in Fig. 10. The positions of the maxima and minima of the cross sections are reproduced by the calculations. There is also general agreement in the magnitudes of the predicted and experimental cross sections. The main difference is in the relative depths of the first and second minima. The calculations predict the first minimum to be deeper than is experimentally observed and the second minimum to be shallower.

The results for 12–21-MeV protons scattered from B^{11} are shown in Fig. 11. With respect to both the magnitudes of the cross sections and the positions of their maxima and minima, calculation and experiment agree well over the entire energy range covered by the data. At low energies, the calculations predict a slightly deeper first minimum than is observed. The worst fit is for the 12-MeV cross sections, for which the position of the second minimum is not reproduced.

Differential cross sections for 12-50-MeV protons scattered from C^{12} are shown in Fig. 12. For energies above 17 MeV, the calculated differential cross sections

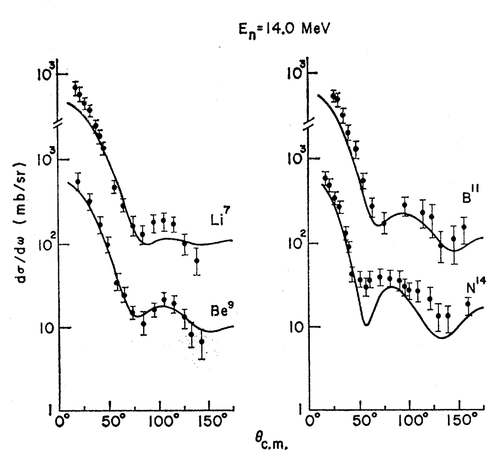

FIG. 14. Differential cross sections for 14-MeV neutrons scattered from Li^7, Be^9, B^{11}, and N^{14} compared with the optical-model calculations.

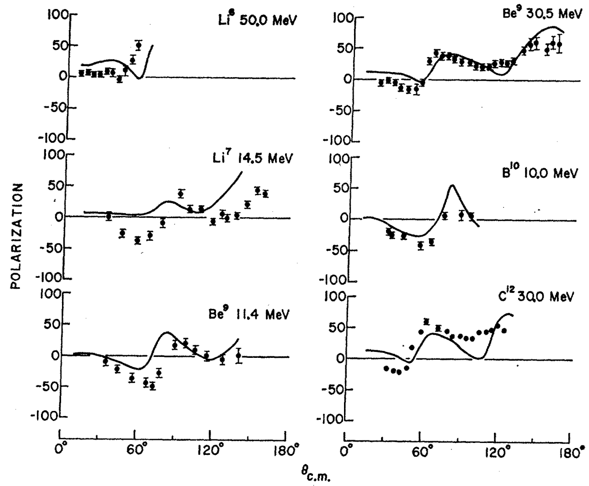

FIG. 15. Polarization of protons scattered from Li^6, Li^7, Be^9, B^{10}, and C^{12} compared with the optical-model calculations.

agree well with the experimental ones; and over the whole energy range, the position of the first minimum is reproduced. Below 17 MeV, the calculations have two minima in the cross sections whereas only one is observed. At 17.8 and 19.4 MeV, the predicted cross sections are lower than experimentally observed but the angular patterns are well reproduced. The fits of the present work are not usually as good as those of the work of Nodvik *et al.*,[5] but their parameters were not constrained to vary smoothly with energy. For bombarding energies between 30 and 50 MeV, the overall shape and magnitude of the experimental cross sections are reproduced by the calculations but the minima in the optical-model calculations are sharper than those in the experimental cross sections.

The calculations for 10–50-MeV protons scattered from N^{14} and O^{16} are shown in Fig. 13. For N^{14}, the positions of the maxima and minima are reproduced by the calculations but the predicted cross sections at 10 and 20 MeV are lower than those experimentally observed. The calculated cross section at 31 MeV is in good agreement with the experimental cross section. The oxygen cross sections are reproduced by the calculations except for the position for the minima observed at 125°. As with all of the cases that have been examined here, the experimental cross sections have somewhat less pronounced structure than is predicted by the optical-model calculations.

In Fig. 14 are shown the experimental cross sections for 14-MeV neutrons elastically scattered from Li^7, Be^9, B^{11}, and N^{14}. The general features are reproduced by the calculations. An interesting feature is that the differences between calculation and experiment are the same as those for proton scattering in this energy range. The angular distributions predicted by the optical model for both protons and neutrons scattered from Be^9 for a bombarding energy of 14 MeV show less pronounced structure than is experimentally observed. For N^{14}, the predicted angular distributions for both elastically scattered protons and elastically scattered neutrons show much deeper minima than are experimentally observed.

Proton polarization data for several $1p$-shell nuclei are compared with the optical-model calculations in

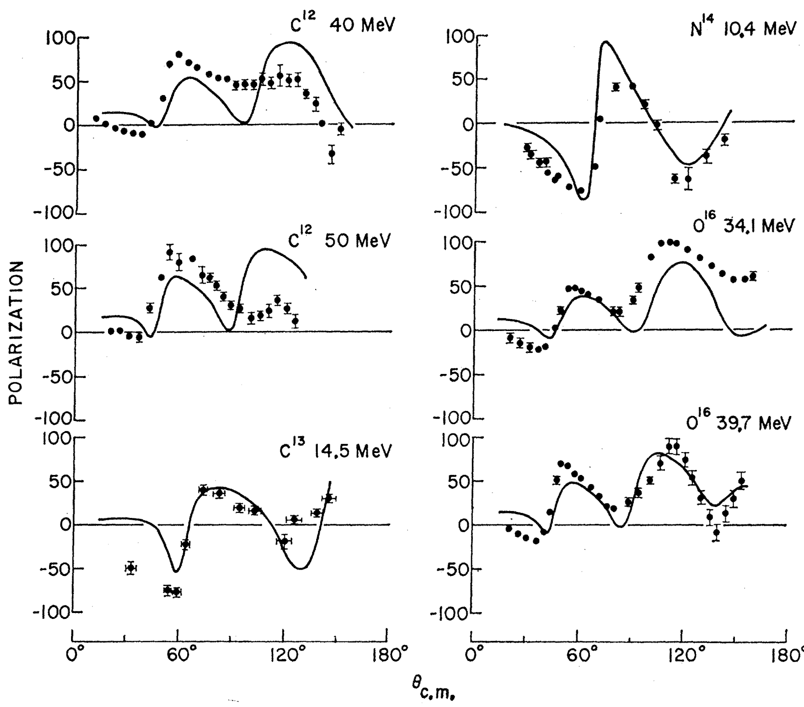

FIG. 16. Polarization of protons scattered from C^{12}, N^{14}, and O^{16} compared with the optical-model calculations.

TABLE II. Comparison between optical-model parameters suggested in the present work and those found by Perey (Ref. 1) and by Fricke *et al.* (Ref. 3.).

Author	V_R (MeV)	W_S (MeV)	W_V (MeV)	V_{so} (MeV)	a_R (F)	a_I (F)	a_{so} (F)	Radius parameters (F)
Perey[a]	$53.3-0.55E$[b] $+0.4\,Z/A^{1/3}$ $+27\,(N-Z)/A$	13.5 ± 2	None	7.5	0.65	0.47	0.65	$r_R=r_I=r_{so}$ $=1.25$
Fricke *et al.*[c]	$49.9-0.22E$[b] $+0.4\,Z/A^{1/3}$ $+26.4\,(N-Z)/A$	Variable	2–4	6.04	0.75	0.63	0.738	$r_R=1.16$ $r_I=1.37$ $r_{so}=1.064$
Present work	$60.0-0.30E$[d] $+0.4\,Z/A^{1/3}$ $+27\,(N-Z)/A$	$0.64E$ for $E<13.8$; $9.6-0.06E$ for $E\geq13.8$	0 for $E<32.7$; $(E-32.7)\times1.15$ for $32.7\leq E\leq39.3$ 7.5 for $E>39.3$	5.5	0.57	0.50	0.57	$r_R=r_I=r_{so}$ $=1.15-0.001E$

[a] Reference 1.
[b] All references to energy refer to the laboratory energy of the incident particle and are in MeV.
[c] Reference 3.
[d] References to energy refer to c.m. energy of the incident particle in MeV.

Figs. 15 and 16. In the cases of Li^6 and Li^7 and for Be^9 at 11.4 MeV, the experimental and calculated polarizations are in poor quantitative agreement, but agree well on the over-all shape of the curves. In the rest of the data, B^{10} through O^{16} at energies between 10 and 50 MeV, the trends with mass and energy are reproduced. The positions of maxima and minima in the polarizations are reproduced but the predicted magnitudes often disagree with the experimental measurements. In all cases, the calculations predict a higher polarization at forward angles than is experimentally observed.

To summarize, when the optical-model parameters suggested in the present work are used the main features of the nucleon elastic scattering data, differential cross sections as well as polarizations, on the nuclei from Li^6 to O^{16} are correctly predicted. However, there are two major discrepancies. First, the manitudes of the experimental and predicted cross sections often differ; but the ~15% uncertainties associated with absolute normalization of major portion of these data renders many of these differences of dubious significance. Second, for bombarding energies above 25 MeV the predicted cross sections generally have sharper structure than do the experimental cross sections. The fact that the resolution width for some of the measurements was much less than 4° indicates that this effect at least partially reflects an inadequacy in the calculation.

V. COMPARISON WITH OTHER PRESCRIPTIONS

Perey[1] has performed an optical-model analysis for angular distributions of protons scattered from several nuclei between Al^{27} and Au^{197} for bombarding energies between 9 and 22 MeV. Fricke, Gross, Morton, and Zucker[3] have carried out a similar analysis for nuclei between Si^{28} and Pb^{208} for proton bombarding energies between 30 and 40 MeV. In Table II, these sets of parameters are compared with the set found in the present work. While these are by no means the only analyses of this type, they are representative of the work done in this area and provide a worthwhile basis for comparison with the parameters determined in the present study. The fits in these other analyses[1,4] are usually better than those of the present work; however, the energy range covered in the other analyses[1,4] is much narrower than that covered here.

The prescriptions for the parameters of the real central potential used in the present analysis give optical-model parameters that are comparable to those obtained with other prescriptions. For the energy range covered in Perey's analysis,[1] the value of the product $V_RR_R^2$ in the present investigation is the same within 2% as that from Perey's prescription.[1] His value of 0.65 F for the diffuseness of the real well is close to the value used in the present analysis. The product $V_RR_R^2$ obtained with the prescription of Fricke *et al.*[3] is within 4% of the value in the present analysis over the energy range 30–40 MeV. An energy dependence associated with the radius parameter of the real central potential is unique to this investigation. As explained above, however, this is not an unexpected result for light nuclei.

The form of the prescription for the strength of the real central potential is the same as that of Perey[1] although the constants involved are different. A qualitative estimate of the uncertainty associated with the strength of the real central potential[8] was obtained by determining the change in V_R required to change the position of the first minima of the predicted cross sections by 3°. This criterion was chosen in view of the fact that the parameters suggested in the present study reproduced the position of the first minimum in the differential cross section of almost every nuclide studied. Keeping all other parameters fixed, a 2-MeV change in V_R shifted the angular position of the first minimum by about 3°. The contribution of the term $(0.4Z/A^{1/3})$ is small and cannot be determined in the

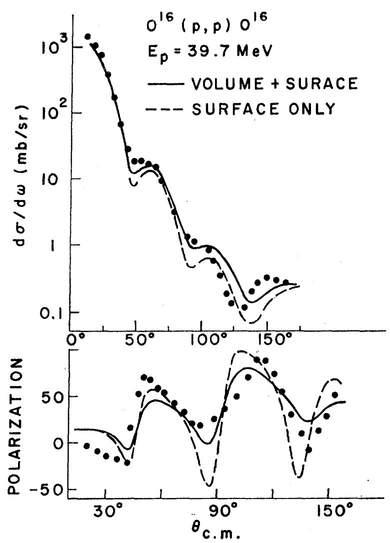

FIG. 17. Cross section and polarization calculated with a purely surface imaginary potential (dashed line) and that for a combination of surface and volume imaginary potentials as suggested in the present analysis (solid line) compared with the experimental data (points).

present investigation. For Li^7, $0.4Z/A^{1/3}=0.63$ MeV while for O^{16} the value is 1.27 MeV. The 0.64-MeV difference is much less than the uncertainty associated with the determination of V_R. For heavy nuclei, other authors[1,2] have found this term to be required. It therefore was included in order that calculations for heavy nuclei can eventually be performed with the parameters used in the present work. The value of the term proportional to $(N-Z)/A$ was chosen from the results of Perey's analysis[1] and no attempt was made to find another value since it seemed to give results consistent with the experimental data.

With the same criterion as in the case of the strength of the real central potential, changing r_R by 0.02 F shifted the position of the first minimum in a predicted cross section by about 3°. The coefficient of $E_{c.m.}$ in the prescription for r_R is determined to within ±50%.

The value of the strength of the spin-orbit potential used in this analysis is less than the 7.5 MeV used by Perey.[1] The value $V_{so}=6.04$ MeV used in the analysis of Fricke *et al.*[3] is near the value 5.5 MeV found in the present analysis.

The behavior of the imaginary potential is not entirely unexpected.[4] At low energies, only the elastic channel is open so that the potential is purely real. As the incident-nucleon energy increases, other channels open up and, hence, a small imaginary component must be added to the potential. As the energy increases further, the number of open channels increases exponentially so that imaginary potential tends to increase and then level off.[5] The asymptotic value of 8 MeV found in the present analysis is smaller than the 13.5 MeV used by Perey.[1] The need for a volume contribution to the imaginary potential for bombarding energies above 30 MeV has been observed in other studies.[3,20] It has an appreciable effect on the predicted polarizations as well as differential cross sections. In Fig. 17, a calculation with a purely surface imaginary potential (dashed line) is compared with that using both a volume and a surface potential (solid line) for protons scattered from O^{16} at 39.7 MeV. When a purely surface imaginary potential was used, the strength of 20 MeV required to fit the experimental cross section worsens the agreement between the calculated and experimental polarization to some extent.

There is evidence[21,22] that an isotopic-spin term is needed in the strength of the imaginary potential. In the present analysis, the strength of the $(N-Z)/A$ term was set by requiring that the magnitudes of the Be^9, B^{10}, and B^{11} cross sections be fitted. A test of this term is its ability to predict the correct magnitude of the elastic neutron scattering cross sections since the sign of the $(N-Z)/A$ term is reversed for neutron scattering. The effect of not reversing the sign of this term in the strength of the imaginary potential is shown in Fig. 18. The inclusion of this term seems to ensure that the fit for neutron scattering is about as good as that for proton scattering. Although these results are not conclusive in themselves, they certainly favor an isotopic-spin term in the strength of the imaginary potential.

VI. CONCLUSIONS

The present analysis shows that the optical model can give a good description of the general features of nucleon scattering from light nuclei. This is evidenced by the fact that, to a fair degree, a single set of energy-

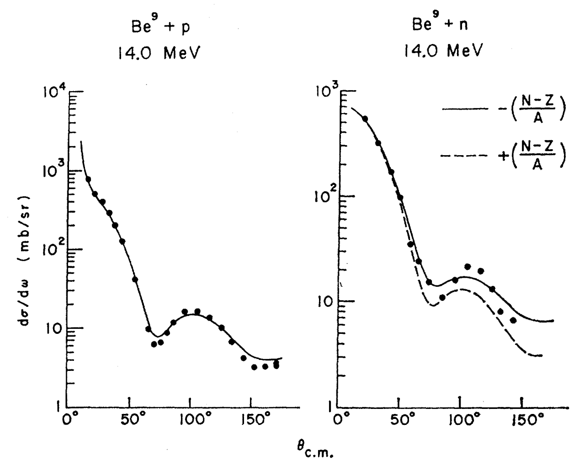

FIG. 18. Comparison between the calculated neutron cross section for Be^9 with (solid curve) and without (dashed curve) reversal of the sign of the $(N-Z)/A$ term in W_s. The points represent the experimental data. Fit for proton scattering from Be^9 at 14.0 MeV is shown on the right for comparison.

[20] G. R. Satchler, Nucl. Phys. **A92**, 273 (1967).
[21] G. R. Satchler, Nucl. Phys. **A91**, 75 (1967).
[22] See discussion and list of references in the review by J. P. Schiffer, J. Phys. Soc. Japan Suppl. **24**, 319 (1968).

dependent parameters is able to reproduce the differential cross sections and polarizations of elastically-scattered protons and neutrons from $1p$-shell nuclei. The set of parameters has characteristics similar to the sets of parameters that fit elastic scattering data for heavier nuclei. The numerical systematics of the model differ somewhat between light and heavy nuclei. The Thomas form of the spin-orbit potential has a peculiar behavior for light nuclei which is compounded by the fact that at low energies the calculations are particularly sensitive to its strength. Over a large energy range, the radius parameter must be energy-dependent; and this dependence cannot be compensated by an increased energy dependence in the real potential. These differences, while small, seem to be significant.

It should be pointed out that the parameters of the present analysis are not necessarily the best set of parameters since they were not determined by a rigorous parameter search. The analysis does indicate that such an analysis would be meaningful. While the data used in the present analysis cover a wide range of energies, the measurements were not spaced at regular intervals over this energy range. When a more complete set of data becomes available, a more rigorous analysis can be undertaken.

ACKNOWLEDGMENTS

The authors would like to thank Dr. R. H. Siemssen for many helpful discussions and for access to unpublished data. One of us (B.A.W.) is indebted to Associated Midwest Universities for their support in the form of a predoctoral fellowship throughout this work.

PHYSICAL REVIEW VOLUME 182, NUMBER 4 20 JUNE 1969

Three-Particle Channels in Nuclear-Reaction Theory*

W. TOBOCMAN

Physics Department, Case Western Reserve University, Cleveland, Ohio 44106

(Received 26 February 1969)

A new approach to the treatment of three-body channels in nuclear-reaction theory is proposed. The method is based on the R-matrix formalism. Instead of introducing three-particle final states as a new class of channels, it is suggested that they be described in terms of incoherent contributions from the various two-body channels having scattering-state residual-nucleus wave functions instead of the customary bound-state ones. The method is (a) illustrated with a simple one-dimensional three-body system, (b) applied to a general three-body system, and finally (c) used to set up a distorted-wave Born-approximation analysis of the general three-body system.

I. INTRODUCTION

FOR the most part, theoretical treatments of scattering and reactions have been restricted to the regime of two-body channels. While some efforts have been made to find the appropriate three-body channel generalizations,[1] useful methods of general applicability have not been forthcoming.

In this paper, we outline a new approach to the description of three-body channels which appears to be at once practical and completely rigorous. We propose to describe three-particle final states in terms of incoherent contributions from two-body channels for which the internal motion of one of the residual nuclei is a scattering state rather than a bound state. Thus, we do not find it necessary to introduce into the R-matrix formalism[2] a new class of three-particle channels to supplement the usual two-particle ones.

A preview sketch of our method is presented in Sec. II. In Sec. III, we demonstrate the method on a simple one-dimensional three-body system. A general three-particle system is treated in Sec. IV. In Sec. V, we show how our analysis of the three-particle scattering problem can provide the basis for a distorted-wave Born-approximation (DWBA) calculation.

II. PREVIEW OF METHOD

The basis of our analysis is the conventional R-matrix theory scheme for defining channels. The $(3N-3)$-dimensional relative-motion configuration space of a given N nucleon system is separated into an "inside region" and an "asymptotic region" by a large closed $(3N-4)$-dimensional hypersurface, the boundary hypersurface, centered at the center of mass. For the purposes of this analysis, this surface will be taken to be arbitrarily large. When the energy of the system is sufficiently small, the wave function will be found to be negligible everywhere on this boundary surface except at certain small patches. Each such patch corresponds to a partition of the N nucleons into two widely separated clusters. Take the boundary hypersurface to be

* Work supported by the U.S. Atomic Energy Commission.

[1] E. Gerjuoy, Ann. Phys. (N.Y.) **5**, 58 (1958); M. Danos and W. Greiner, Z. Physik **202**, 125 (1967); F. S. Levin, Ann. Phys. (N.Y.) **46**, 41 (1968).

[2] A. M. Lane and R. G. Thomas, Rev. Mod. Phys. **30**, 257 (1958); L. Garside and W. Tobocman, Phys. Rev. **173**, 1047 (1968).